

## ARTICLE

# Purification effects show seed and root mucilage's ability to respond to changing rhizosphere conditions

Doerte Diehl  | Mathilde Knott | Gabriele E. Schaumann 

Environmental and Soil Chemistry Group,  
Rheinland-Pfälzische Technische Universität  
Kaiserslautern Landau, RPTU in Landau,  
iES Institute for Environmental Sciences,  
Landau, Germany

**Correspondence**

Doerte Diehl, Environmental and Soil  
Chemistry Group, Rheinland-Pfälzische  
Technische Universität Kaiserslautern Landau,  
RPTU in Landau, iES Institute for  
Environmental Sciences, Fortstrasse 7 76829  
Landau, Germany  
Email: [d.diehl@rptu.de](mailto:d.diehl@rptu.de)

**Funding information**

Deutsche Forschungsgemeinschaft,  
Grant/Award Number: 403668613

**Abstract**

Mucilage, a polysaccharide-containing hydrogel, is hypothesized to play a key role in the rhizosphere as a self-organized system because it may vary its supramolecular structure with changes in the surrounding solution. However, there is currently limited research on how these changes are reflected in the physical properties of real mucilage. This study examines the role of solutes in maize root, wheat root, chia seed, and flax seed mucilage in relation to their physical properties. Two purification methods, dialysis and ethanol precipitation, were applied to determine the purification yield, cation content, pH, electrical conductivity, surface tension, viscosity, transverse  $^1\text{H}$  relaxation time, and contact angle after drying of mucilage before and after purification. The two seed mucilage types contain more polar polymers that are connected to larger assemblies via multivalent cation crosslinks, resulting in a denser network. This is reflected in higher viscosity and water retention ability compared to root mucilage. Seed mucilage also contains fewer surfactants, making them better wettable after drying compared to the two root mucilage types. The root mucilage types, on the other hand, contain smaller polymers or polymer assemblies and become less wettable after drying. However, wettability not only depends on the amount of surfactants but also on their mobility, as well as the strength and mesh size of the network structure. The changes in physical properties and cation composition observed after ethanol precipitation and dialysis suggest that the polymer network of seed mucilage is more stable and specialized in protecting the seeds from unfavorable environmental conditions. In contrast, root mucilage is characterized by fewer cationic interactions and its network relies more on hydrophobic interactions. This allows root mucilage to be more flexible in responding to changing environmental conditions, facilitating nutrient and water exchange between root surfaces and the rhizosphere soil.

**KEYWORDS**

cations, hydrogel, repellency, root mucilage, surface tension, viscosity

This is an open access article under the terms of the [Creative Commons Attribution](https://creativecommons.org/licenses/by/4.0/) License, which permits use, distribution and reproduction in any medium, provided the original work is properly cited.

© 2023 The Authors. *Biopolymers* published by Wiley Periodicals LLC.

## 1 | INTRODUCTION

### 1.1 | Root mucilage

Plants engineer their root environments by secreting a variety of substances to alter their surrounding conditions in response to environmental stresses. Considering the rhizosphere as a self-organized system,<sup>[1]</sup> we expect that root and seed exudates will play a key role in this system. Mucilage exuded by roots or seeds is a mixture of low and high-molecular-weight compounds dominated by polysaccharides with hydrogel properties, allowing for an enormous water holding capacity. Earlier studies have shown that root mucilage can modulate water content dynamics in the rhizosphere.<sup>[2-4]</sup> For instance, soil covered with mucilage may become hydrophobic after drying.<sup>[3,5,6]</sup> One possible explanation is that surface-active substances, such as phospholipids exuded by plant roots, accumulate at the mucilage-air interface during drying, making the soil surface hydrophobic.<sup>[7]</sup> Additionally, changes in the supramolecular structure during drying might lead to an orientation of hydrophilic functional groups towards the inside of the mucilage phase, while hydrophobic parts tend to orient outward towards the air. The extent of these changes during drying and the retardation of the rewetting and reswelling process probably depend on the type and strength of polymer-polymer interactions, as well as polymer-water interactions.

### 1.2 | Supramolecular interactions in mucilage

The dynamics of the supramolecular structure of polysaccharides relies on physical (non-covalent) inter- and intramolecular cross-linkages, such as ionic and electrostatic interactions, hydrogen bonding, complexation, or hydrophobic interactions.<sup>[8]</sup> These interactions can be modified by changes in the surrounding soil solution, such as pH and the concentrations of mono- and multivalent inorganic and organic cations and anions,<sup>[9,10]</sup> as well as the size distribution and concentration of the polymers themselves. Consequently, the modifications of the supramolecular polymer structure are hypothesized to underlie self-assembling mechanisms,<sup>[11]</sup> occurring spontaneously in response to changes that minimize the energetic state of the mucilage structure. The presence of multivalent cations mediates electrostatic interactions,<sup>[12]</sup> and the number of deprotonated acidic groups in acidic polysaccharides affects these interactions.<sup>[13]</sup> Therefore, the physical properties of electrostatically stabilized mucilage are expected to significantly change after the removal of multivalent cations and with changes in pH. Hydrogen bonding in polysaccharides is based on hemiacetal oxygen, hydroxyl, or methyl groups of the sugar residues,<sup>[14]</sup> and it is also pH-dependent due to the protonation of carboxylic acid groups.<sup>[15]</sup> Lastly, the rather weak hydrophobic interactions in mucilage are particularly challenging to investigate because their strength does not rely on the attraction between nonpolar groups but rather on the minimum potential energy state of the system. These interactions come into play when non-polar groups, such as O-acetyl, O-methyl substituents, or covalently bonded hydrophobic proteins, interact with each other.<sup>[16]</sup> Studies with polyacrylamide hydrogels formed via hydrophobic interactions with stearyl groups have shown that in the presence of surfactants, more hydrophobic interactions dissociate under

force compared to the absence of surfactants.<sup>[17]</sup> This disengagement was reversible to nearly 100% in the presence of surfactants, while no such “self-healing” behavior was observed without surfactants.<sup>[17]</sup> Therefore, hydrogels stabilized by hydrophobic interactions are expected to change their physical properties upon the release of surfactants.

### 1.3 | Physicochemical gel properties depending on supramolecular structure

Changes in the supramolecular arrangement of molecules in mucilage are reflected in its physical properties, such as viscosity, surface tension, water retention in the network, and wettability. Viscosity increases with a higher degree and strength of polymer-polymer interactions, molecular size, the strength of electrostatic attraction between oppositely charged groups or cross-links, and the entanglement of molecule chains.<sup>[18]</sup> The transverse proton relaxation time ( $T_2$  relaxation time) in hydrogels primarily describes the spin-spin relaxation of protons in the solvent water.<sup>[19]</sup> The  $T_2$  time depends on the solid concentration and the supramolecular arrangement of the polymers, including the form and mesh size of the three-dimensional network formed by the polymers.<sup>[13]</sup> Therefore, the  $T_2$  relaxation time decreases with a more restricted water environment, corresponding to a smaller mesh size of the network. Hence, we anticipate that the network stabilizing effects on mucilage, expressed as increased viscosity, will also decrease the  $T_2$  relaxation time.

With increasing concentration, amphiphiles accumulate at the water-air interface until a complete surface film is formed. Further increasing the concentration leads to the formation of micelles or interactions with hydrophobic sites within the liquid phase. During drying, amphiphiles can render a surface hydrophobic by arranging the hydrophobic part towards the air. Thus, we expect that the removal of small soluble LMW substances from the mucilage during dialysis would significantly increase the surface tension and improve wettability after drying. However, wettability depends not only on the type of surface molecules but also on how quickly they can reorient during drying and rehydration. It also depends on the type and number of inter- and intramolecular interactions in several upper molecular layers.<sup>[20]</sup> These physical properties determine the spatial patterns of mucilage and, consequently, affect wettability, hydraulic properties, and transport processes in the rhizosphere under changing environmental conditions (e.g., water content, pH, presence of mono- and multivalent cations, and surface-active substances such as dissolved organic matter).

### 1.4 | Objectives and experimental approach

The present study aims to understand the role of solutes, particularly cations and surface-active substances, in influencing changes in key physical properties of mucilage under varying environmental conditions that have a known impact on the diverse functions of mucilage in the rhizosphere. To achieve this, we analyzed the effects of two contrasting purification methods: dialysis and ethanol precipitation. Depending on the availability of cations, the presence of surfactants, the charge and

size of the polymers, and their intermolecular interactions, we anticipated different effects of the purification treatments on purification yield, as well as the physical and physicochemical properties.

## 2 | MATERIALS AND METHODS

### 2.1 | Mucilage collection and storage

For the present study, mucilage from chia seeds (*Salvia hispanica*, dm-drogerie markt GmbH+Co. KG, Germany, produced in India, L9910303, AT-BIO-301) and flax seeds (*Linum usitatissimum* L., dm-drogerie markt GmbH+Co. KG, Germany, produced in Paraguay), as well as mucilage from maize roots (*Zea mays*, KWS 2376, KWS Lochow GmbH, Germany) and wheat roots (*Triticum aestivum*, WIWA ZS, BayWa AG, Germany), were produced, purified, and analyzed. Root mucilage was produced aeroponically following the detailed method described in Brax et al.<sup>[21]</sup> Briefly, the seeds were initially treated with 10% H<sub>2</sub>O<sub>2</sub> to prevent mold development, washed in distilled water, and then placed on a stainless-steel mesh in a water-saturated atmosphere in darkness for 1 week. After 3–4 days, seedlings began to grow, and mucilage drops at the root tips were harvested daily for the following 3–4 days and stored frozen. Once the desired amount of root mucilage was collected, it was thawed, filtered through a 100 µm stainless steel sieve, freeze-dried, and stored at –20°C.

Seed mucilage was produced by mixing the seeds with 15 mL of ultrapure water per gram of chia seeds and 6 mL per gram of flax seeds. After a swelling time of 2 h for chia seeds and 6 h for flax seeds, the seeds and mucilage were separated first using a 500 µm sieve, and then a 100 µm stainless steel sieve. The separated mucilage was then freeze-dried and stored at –20°C. For all subsequent experiments, freeze-dried purified or untreated mucilage was rehydrated in ultrapure water at a concentration of 3 mg of mucilage per gram of water (0.3 weight%) over 2 days under gentle shaking in a refrigerator.

### 2.2 | Purification by dialysis and ethanol precipitation and yield of purification

For dialysis, approximately 20–30 g of mucilage (0.3 weight%) of each type was filled into pre-cleaned cellulose dialysis tubing (Sigma-Aldrich, Steinheim, Germany, MW cut-off 12–14 kDa), sealed with clamps, and placed in a 2 L beaker filled with ultrapure water. The water was replaced every 24 h after measuring the pH and electrical conductivity (EC) using a Consort C863 pH/EC meter (Consort nv, Turnhout, Belgium). After 96 h, the samples were freeze-dried using a Christ Alpha 1-2 LDplus freeze dryer (Christ, Osterode, Germany), and then weighed to determine the purification yield.

For ethanol precipitation, 10 mL of mucilage (0.3 weight%) was mixed with 40 mL of 99.8% ethanol (Rotipuran® ≥99.8%, p.a., Carl Roth, Karlsruhe, Germany) in an ice bath on a shaking platform for 2 h. The mixture was then centrifuged at 4193 RCF for 20 min using a Hettich Centrifuge (Universal 320, Tuttlingen, Germany). The

mucilage pellet was subjected to two additional 1-hour incubations in an ice bath on the shaking platform with 40 mL of fresh 99.8% ethanol, followed by centrifugation for 15 min at 4193 RCF. The ethanol supernatant was discarded, and after washing, the pellet was dissolved in 20 mL of ultrapure water. The dissolved mucilage was then freeze-dried and weighed to determine the purification yield. Three fractions based on molecular size and solubility were calculated from the purification yield using Equations (1)–(3).

$$F1 = 1 - \text{yield}_{(\text{EtOH})}, \quad (1)$$

$$F2 = \text{yield}_{(\text{EtOH})} - \text{yield}_{(\text{dialysis})}, \quad (2)$$

$$F3 = \text{yield}_{(\text{dialysis})}. \quad (3)$$

Fraction F1 (small-soluble) represents the ethanol (EtOH) soluble fraction consisting of molecules or assemblies smaller than 12–14 kDa. Fraction F2 (small-insoluble) is the EtOH insoluble fraction with molecules or assemblies smaller than 12–14 kDa, while fraction F3 (large-insoluble) is the EtOH insoluble fraction primarily composed of molecules or assemblies larger than 12–14 kDa.

Samples were rehydrated in ultrapure water to a concentration of 0.3 weight%, and pH, EC, and the following parameters were measured.

### 2.3 | Cation content

To determine the cation content, 1 mL of the hydrated mucilage sample was digested with 0.5 mL of HCl (ROTIPURAN® ≥32%, p.a., Carl Roth, Karlsruhe, Germany) and 1.5 mL of HNO<sub>3</sub> (ROTIPURAN® ≥65%, p.a., Carl Roth, Karlsruhe, Germany) using a microwave. The digestion process involved a 15-minute heating ramp followed by constant heating at 200°C for 40 min. The digests were diluted and analyzed using inductively coupled plasma optical emission spectrometry (ICP-OES, Agilent 720 Series, Germany) to determine the concentrations of metals such as Al, Fe, Ca, Mg, Na, and K. The results were then normalized to the dry mass of the digested mucilage and expressed as millimoles of charge (mmol<sub>c</sub>) per gram of dry mass.

To evaluate the balance of cations between retained and removed fractions and their distribution across different size and solubility fractions, all contents were also related to the original mass of non-treated mucilage (NT) using the purification yield, and expressed as mmol<sub>c</sub> per gram of NT. Since the yield could only be determined without replicates, small errors were strongly propagated, particularly for the very small contents of trivalent ions. This led to calculated increases in cation contents upon treatment that were impossible in reality. To address this, for dialyzed and ethanol-precipitated chia seed mucilage, as well as ethanol-precipitated wheat mucilage, the smallest theoretically possible yield that caused no virtual accumulation was calculated and averaged with the measured yield. To visualize these

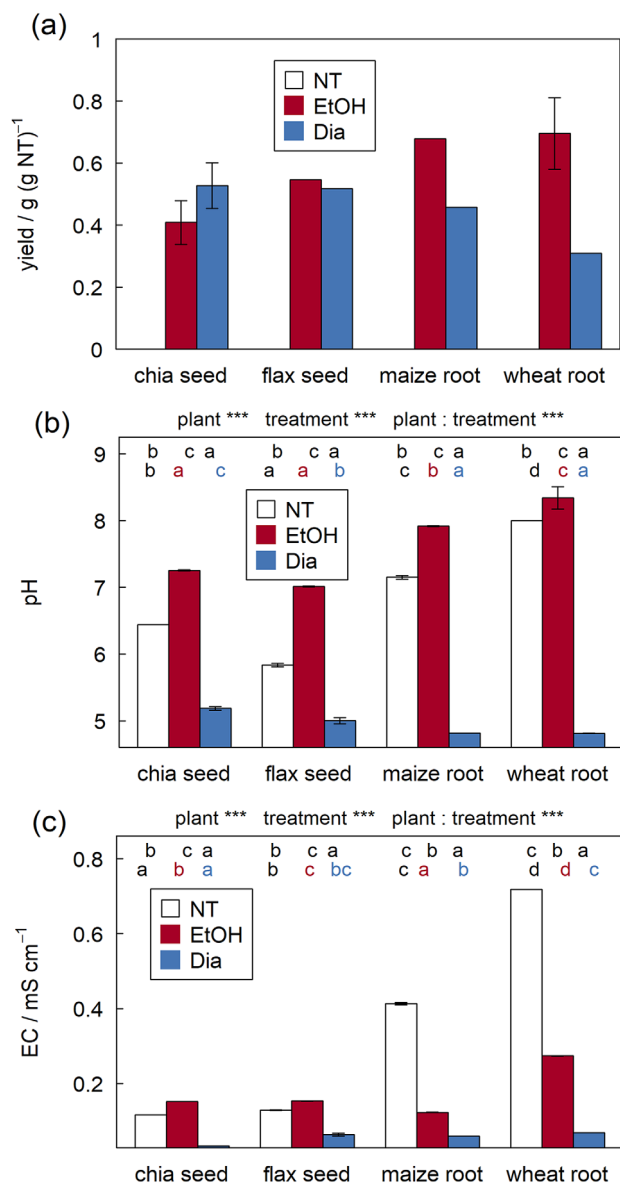


**FIGURE 1** (a) Purification yield relative to the deployed non-treated dry mass, (b) pH and (c) electrical conductivity (EC) of non-treated mucilage (NT) and mucilage purified by dialysis (Dia) or by ethanol precipitation (EtOH) of chia and flax seeds and maize and wheat roots. Same letters above the bars in the first line indicate no significant differences between treatments of mucilage of the same plant, while same letters in the same color in the second line indicate no significant differences between mucilage of different plants of the same treatment. Error bars represent standard errors of replicates. The origin of error bars in (a) are explained in 2.3. As NT samples were not purified, their yield is not shown.

modifications, the measured and calculated values are represented by the upper and lower ends of error bars, respectively, as shown in Figures 1a and 2c.

Finally, the cations belonging to each size/solubility fraction were calculated using Equations (4)–(6) to describe the non-treated mucilage (NT), and related to the yield of the respective treatment to describe the treated mucilage. Specifically,  $c_{(\text{cation},F2)}$  and

$c_{(\text{cation},F3)}$  were divided by  $\text{yield}_{(\text{EtOH})}$ , and  $c_{(\text{cation},F3)}$  was divided by  $\text{yield}_{(\text{Dia})}$ .

$$c_{(\text{cation},F1)} \left[ \text{mmol}_c \text{ cation } (\text{g NT})^{-1} \right] = \frac{n_{(\text{cation},F1)}}{m_{(\text{dry},\text{NT})}} = \frac{n_{(\text{cation},\text{NT})}}{m_{(\text{dry},\text{NT})}} - \frac{n_{(\text{cation},\text{EtOH})}}{m_{(\text{dry},\text{NT})}}, \quad (4)$$

$$c_{(\text{cation},F2)} \left[ \text{mmol}_c \text{ cation } (\text{g NT})^{-1} \right] = \frac{n_{(\text{cation},F2)}}{m_{(\text{dry},\text{NT})}} = \frac{n_{(\text{cation},\text{EtOH})}}{m_{(\text{dry},\text{NT})}} - \frac{n_{(\text{cation},\text{Dia})}}{m_{(\text{dry},\text{NT})}}, \quad (5)$$

$$c_{(\text{cation},F3)} \left[ \text{mmol}_c \text{ cation } (\text{g NT})^{-1} \right] = \frac{n_{(\text{cation},F3)}}{m_{(\text{dry},\text{NT})}} = \frac{n_{(\text{cation},\text{Dia})}}{m_{(\text{dry},\text{NT})}}. \quad (6)$$

## 2.4 | Viscosity

Flow measurements were conducted in triplicate at 20°C using a rheometer (MCR 102, Anton Paar, Ostfildern, Germany) with a cone plate (CP50-1, diameter = 50 mm; angle of 1°). Each replicate consisted of a 600  $\mu\text{L}$  sample, with a gap of 0.1 mm and shear rates ranging from 0.001 to 1000  $\text{s}^{-1}$  in seven logarithmic steps. For statistical analysis, the apparent viscosity at 1  $\text{s}^{-1}$  was compared for all samples and treatments since low-shear viscosity is more relevant for the dynamic behavior of mucilage in the rhizosphere.

## 2.5 | <sup>1</sup>H-NMR transverse proton relaxation time $T_2$

The transverse proton relaxation time  $T_2$ , which is a measure of the rotational restriction of protons in water within the polymer network, was obtained from <sup>1</sup>H NMR measurements (minispec mq 7.5, Bruker, Rheinstetten, Germany) with three replicates. The transverse relaxation decay was obtained using the Carr-Purcell-Meiboom-Gill (CPMG) pulse sequence<sup>[22]</sup> with 16 scans, a 0.3 ms echo time, 12,000 echoes, a recycle delay of 10 s, and a gain between 80 and 94 dB. Decay curve fitting was attempted using multi-exponential decay equations in R.<sup>[23]</sup> However, only mono-exponential fits provided reasonable results since all additional decays had intensities below 1%.

## 2.6 | Surface tension

Surface tension was measured using the pendent drop method. A disposable 1 mL syringe (Omnifix®-F) equipped with a blunt needle (Sterican® 18G/1.2  $\times$  40 mm, B. Braun Melsungen AG, Melsungen, Germany) was filled with the sample and fixed in the video-based optical contact angle device (OCA15Pro, DataPhysics, Filderstadt, Germany). A hanging drop of 10–20  $\mu\text{L}$  was dosed at the needle end using the dosing unit of the device, and an image was captured. The drop volume was then increased in 0.1  $\mu\text{L}$  steps, with each step captured after a balancing time of 10 s, until the drop fell down within this balancing time. The procedure was repeated for 3–4 replicate drops. The last image with the highest drop volume was evaluated for surface tension using the Pendant Drop plug-in<sup>[24]</sup> of the ImageJ

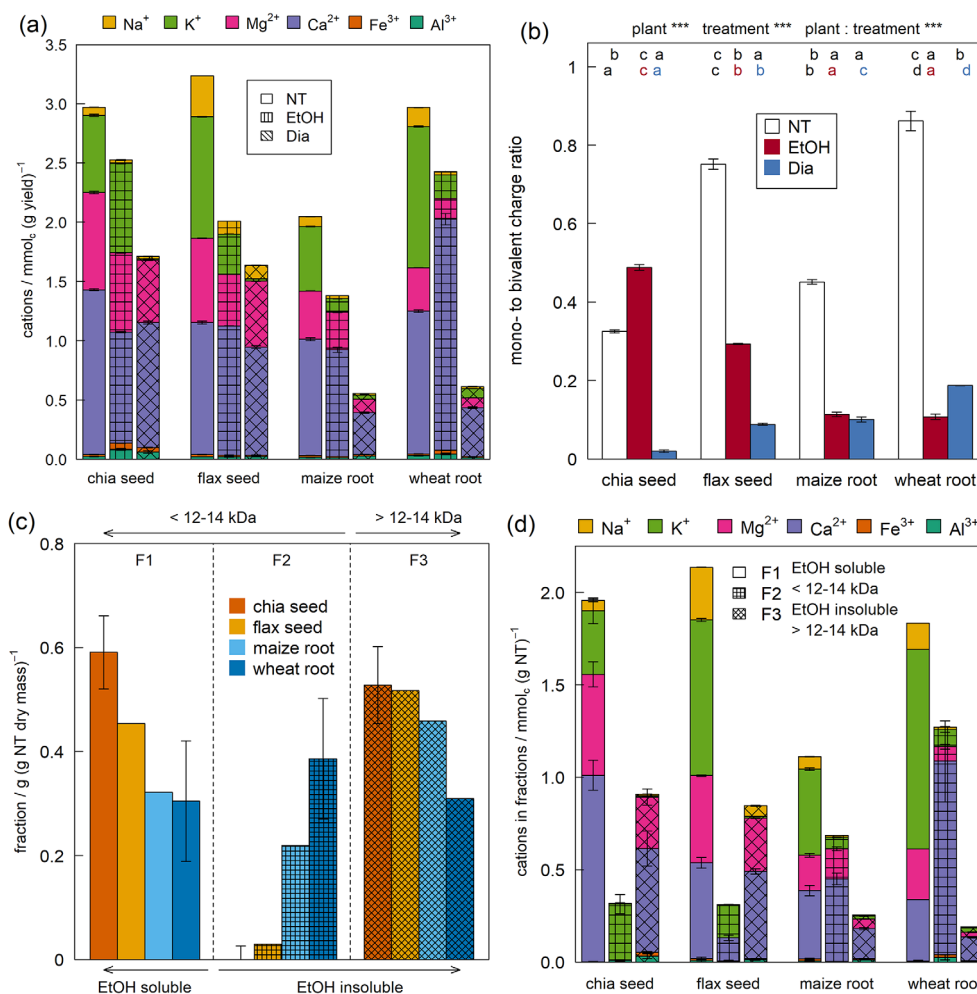


**FIGURE 2** (a) Cation charge composition of non-treated (NT) mucilage and mucilage purified by dialysis (Dia) or by ethanol precipitation (EtOH) for aluminum Al, iron Fe, calcium Ca, magnesium Mg, potassium K, and sodium Na, related to the dry mass, (b) mono- to bivalent cation charge ratio, (c) size and polarity fractions calculated from dialysis and EtOH precipitation yield, and (d) cation charge composition of these fractions related to the dry mass of the non-treated mucilage (NT) for chia and flax seed and maize and wheat root mucilage. Error bars represent standard errors of three replicates.

software,<sup>[25]</sup> taking into account the needle diameter in each picture to set the correct scale of pixels per mm. As equilibrium is likely not reached within 10 s, we must consider that the measured values reflect not only the amount of amphiphiles but also their diffusion time to reach the surface.

## 2.7 | Contact angle

For contact angle measurement, microscope borosilicate coverslips (hydrolytic class I, 24 × 50 mm, Carl Roth, Karlsruhe, Germany) were cleaned for 10 min in acetone, isopropanol, and ultrapure water, dried under N<sub>2</sub>, fixed on a larger specimen holder, and treated for 20 min at 30°C in an ozonizer (Novascan, PSD Pro Series Digital UV Ozone System) to achieve a contact angle below 10° and allow complete spreading of the mucilage sample. Following Kaltenbach et al.,<sup>[26]</sup> mucilage samples were diluted to 1.104 mg mL<sup>-1</sup> (552 μL of 0.3 weight% mucilage filled to 1.5 mL ultrapure water), and 1.5 mL of the diluted samples was spread on the cleaned coverslip, resulting in a

solid concentration of 0.138 mg cm<sup>-2</sup>. After drying at ambient temperature in a desiccator over silica gel for 4 days, changes in the drop shape of sessile drops of 1 μL with respect to spreading time on the dried mucilage layer were recorded by a video-based optical contact angle device (OCA15Pro, DataPhysics, Filderstadt, Germany) over 1 min with five frames per second. On each coverslip, spreading of 5–10 replicate drops was recorded. The contact angle of the drops as a function of drop age was then evaluated using SCA20 software (DataPhysics, Filderstadt, Germany) by circle fitting. For statistical evaluation, the contact angles at a drop age of 1 s were compared for all samples and treatments.

## 2.8 | Statistical evaluations

Results are presented as mean values of replicates with error bars representing standard errors of the replicates. To test the effect of purification and the plant of mucilage origin on the respective

parameter, linear mixed-effects models (LMEM) were fitted to the data, with replicates as random effects, using R<sup>[23]</sup> and the packages “lme4”<sup>[27]</sup> and “lmerTest”.<sup>[28]</sup> First, the interaction of both factors was included: lmer (parameter = plant × treatment + (1|replicate)). If the interaction term was not significant, the test was repeated without the interaction. If one of the factors, either plant or treatment, had no significant effect on the parameter, it was excluded in the last test. Results are indicated above the bar diagrams with “\*\*\*\*” for  $p < 0.001$ , “\*\*\*” for  $p < 0.02$ , “\*\*” for  $p < 0.05$ , and “\*” for  $p < 0.1$ , following the factors “plant”, “treatment”, and “plant:treatment” for the interaction. To test significant differences between the treatments of mucilage of the same plant and between mucilage of different plants with the same treatment, the following tests were applied for subsets of data: lmer (parameter = treatment + (1|replicate))/lmer (parameter = plant + (1|replicate)). For significant effects, multiple pairwise comparisons using the “multcomp” package<sup>[29]</sup> with glht (lmer-model, linfct = mcp (treatment = “Tukey”)) or glht (model, linfct = mcp(plant = “Tukey”)) were conducted. The results were displayed as a compact letter display (cld function) of all pairwise comparisons inside the diagrams for the comparison of mucilage of the same plant (upper line) and with different colors for the comparison of mucilage with the same treatment (second line). The validity of the models was tested for normality and variance homogeneity of the residuals using Shapiro–Wilk–Normality test (shapiro.test) and Levene’s test (levenesTest) from the “car” package.<sup>[30]</sup> If the assumptions of normality and variance homogeneity were not met, data were transformed, for example, by taking the cosine of the contact angle or the logarithm of viscosity and  $T_2$  relaxation time. Correlations between parameters were tested using cor.test for linear regressions. The results include the correlation coefficient  $R^2$  and the  $p$  value. Correlations with  $p$  values smaller than 0.1 were considered indicative of a relationship, while correlations with  $p$  values smaller than 0.2 were considered as trends.

## 3 | RESULTS

### 3.1 | Purification yield, pH and EC of mucilage

The purification yield of dialysis (Dia) was higher for seed mucilage than for root mucilage. It decreased from chia seed to flax seed, maize root, and wheat root mucilage, suggesting the presence of an increasing amount of low molecular weight compounds in the untreated mucilage in this order (Figure 1a). Interestingly, the yield of ethanol precipitation (EtOH) increased in the same order, being higher for seed mucilage than for root mucilage. This indicates that, especially for the two types of root mucilage, a considerable portion of molecules or assemblies with sizes below 12–14 kDa, which were removed from the polymer network during dialysis, was precipitated by ethanol and thus remained after the ethanol treatment.

In the non-treated (NT) mucilage, pH values were lower in seed mucilage than in root mucilage. The pH range was less than 6 for flax seed mucilage, approximately 6 for chia seed mucilage, approximately 7 for maize root mucilage, and around 8 for wheat root mucilage

(Figure 1b). Ethanol precipitation increased the pH to values of 8–8.5 in root mucilage, while pH values in seed mucilage adjusted around 7 (Figure 1b). In contrast, dialysis significantly reduced the pH to a narrower range of values: 4.8 in root mucilage, and 5.0 and 5.2 in flax and chia seed mucilage, respectively.

Electrical conductivity (EC) in the NT samples was significantly lower in seed mucilage compared to root mucilage (Figure 1c). It increased in the same order as the Dia yield decreased and the EtOH yield increased (Figure 1a). Ethanol precipitation slightly but significantly increased EC in seed mucilage to  $0.15 \text{ mS cm}^{-1}$ , whereas EC in root mucilage was significantly reduced by ethanol precipitation, although not as effectively as by dialysis, and likely not independently from the original EC (Figure 1c). In fact, wheat root mucilage, which had the highest original EC, still contained a higher amount of mobile charge carriers than maize root mucilage after the ethanol treatment. Dialysis effectively reduced EC in all mucilage types to values below  $0.1 \text{ mS cm}^{-1}$ , regardless of the original EC in the non-treated mucilage.

## 3.2 | Cations before and after purification

### 3.2.1 | Cation composition in non-treated samples

The total cation content in non-treated samples (NT) mucilage was significantly higher for chia seed, flax seed, and wheat root mucilage ( $\sim 3 \text{ mmol}_c \text{ g}^{-1}$ ) compared to maize root mucilage ( $\sim 2 \text{ mmol}_c \text{ g}^{-1}$ , Figure 2a). The cation composition of all NT mucilage samples was dominated by bivalent cations, particularly calcium (Ca), accounting for over 50% of the charge (Figure 2a). Seed mucilage contained significantly more bivalent cations than root mucilage due to a higher magnesium (Mg) content (Figure 2a; for more details and statistical results, please refer to Supplemental Information Figure S1d). However, NT flax seed and wheat root mucilage had the highest potassium (K) content, nearly double that of NT chia seed and maize root mucilage ( $0.5\text{--}0.6 \text{ mmol}_c \text{ g}^{-1}$ , Figure S1e), resulting in a significantly higher mono- to bivalent cation charge ratio (Figure 2b). Additionally, NT flax seed and wheat root mucilage had elevated sodium (Na) contents. In flax seed mucilage Na content was approximately four times higher ( $\sim 0.35 \text{ mmol}_c \text{ g}^{-1}$ ) compared to NT chia seed and maize root mucilage ( $< 0.1 \text{ mmol}_c \text{ g}^{-1}$ ), while wheat root mucilage had approximately double the Na content ( $\sim 0.15 \text{ mmol}_c \text{ g}^{-1}$ ) (Figure S1f). The contribution of trivalent cations, such as iron (Fe) and aluminum (Al), was very low and did not significantly differ among the four investigated mucilage types (Figure S1a,b).

### 3.2.2 | Cations composition after purification

Ethanol precipitation generally reduced the total cation content. The remaining total amount of cations decreased from EtOH chia seed to wheat root and flax seed, and finally to maize root mucilage (Figure 2a). The two seed mucilage types retained more K during

ethanol precipitation compared to the two root mucilage types (Figure 2a, Figure S1e). Wheat root mucilage retained significantly higher amounts of Ca and lower amounts of Mg than the other mucilage types and even showed enrichment in Ca compared to the NT mucilage (Figures 2a, S1c,d).

Dialysis was significantly more effective in removing cations than ethanol precipitation (Figure 2a). The two seed mucilage types retained significantly more cations after dialysis compared to the two root mucilage types, with approximately  $1 \text{ mmol}_c (\text{g NT})^{-1}$  versus  $0.25 \text{ mmol}_c (\text{g NT})^{-1}$ , respectively (Figure 2a). Dialysis almost completely removed K from seed mucilage, while the dialyzed root mucilage samples still contained a significant amount of K (Figure 2a, Figure S1e). In contrast, seed mucilage types retained significantly higher amounts of bivalent cations compared to root mucilage (Figure 2a, Figure S1c,d).

This contrasting effect of the purification methods on the cation composition was also reflected in the mono- to bivalent charge ratio of cations (Figure 2b). Due to the higher K content, the ratio was higher in the NT mucilage of flax seeds and wheat roots ( $>0.7$ ) compared to chia seeds and maize roots ( $<0.5$ ). Ethanol precipitation increased the mono- to bivalent charge ratio only for chia seed mucilage, while it decreased for the other mucilage types, leading to values decreasing from chia ( $\sim 0.5$ ) to flax seed ( $\sim 0.3$ ) and to maize and wheat root mucilage ( $\sim 0.1$ ) (Figure 1b). In contrast, the ratio after dialysis was strongly reduced for all mucilage types and increased from chia seed mucilage over flax seed and maize root mucilage to wheat root mucilage.

### 3.2.3 | Polarity/size fractions and their cation content

As reported by Yan,<sup>[31]</sup> oligosaccharide components of maltodextrin with a degree of polymerization (DP) greater than 12 are practically insoluble in 80% ethanol. Based on this, we assume that all substances present in the dialysis yield (i.e., greater than 12–14 kDa, equivalent to a DP of glucose of approximately 70–80) were also present in the ethanol precipitation yield. Consequently, three different mucilage fractions that characterize the NT mucilage composition with increasing size and decreasing polarity can be calculated from the purification yields (see Section 2.2). While fraction F1 and F3 decreased from the seed to the root mucilage types, fraction F2 was virtually absent in chia seed mucilage and increased from flax seed to maize and wheat root mucilage (Figure 2c).

Figure 2d shows the cation composition of these three fractions (for statistical comparison, please refer to Figure S2). The “free” cations in F1, which were removed by ethanol precipitation, constitute the largest portion of cations in all mucilage types (Figure 2d). Dialysis-resistant cations in F3 were strongly depleted in monovalent cations. The total amount of cations in F2, and specifically the amount of Ca, increased from chia seed to maize and wheat root mucilage, probably at the expense of Ca in F1, which decreased in the same order. In contrast, K content in F2 decreased from chia seed to maize and wheat root mucilage.

## 3.3 | Physicochemical properties of mucilage

The surface tension of untreated root mucilage was significantly lower than that of untreated seed mucilage (Figure 3a). The effect of ethanol precipitation followed no clear pattern. In contrast, dialysis significantly increased the surface tension of root mucilage, while it did not significantly affect the surface tension of seed mucilage.

The viscosity of untreated mucilage was highest for flax seed and decreased in the order of chia seed, maize root, and wheat root mucilage (Figure 3b). The effect of purification on viscosity differed between the plants. The viscosity of chia seed mucilage was neither significantly affected by dialysis nor by ethanol precipitation. For maize and wheat root mucilage, viscosity significantly increased following dialysis and ethanol precipitation, with even stronger increase following ethanol precipitation in the case of wheat root mucilage. Surprisingly, dialysis significantly decreased the viscosity of flax seed mucilage, while the ethanol-precipitated mucilage of flax seed showed the highest viscosity among all treated samples.

The wettability, expressed as the cosine of the sessile drop contact angle, was lowest for maize root and highest for chia seed mucilage, while it did not significantly differ between flax seed and wheat root mucilage (Figure 3c). The effect of both ethanol precipitation and dialysis was highly plant-specific. Upon ethanol precipitation, wettability significantly decreased for chia seed and wheat root mucilage, while it remained unaffected in maize root mucilage and was slightly but significantly increased in flax seed mucilage. In contrast, dialysis significantly increased the wettability of chia seed and maize root mucilage but did not affect it for flax seed and wheat root mucilage.

$T_2$  relaxation times of mucilage in the range between 1 and 2.5 s reflect a relatively weak and unspecific restriction of the rotational mobility of water protons, such as their interactions with a network formed by the polymers. Therefore, we interpret increasing  $T_2$  relaxation time as increasing water mobility, indicating a lower amount of water retained in the polymer network in the mucilage sample or a looser network with a larger mesh size and thus a weaker restriction of the retained water molecules.<sup>[32]</sup> For the untreated mucilage,  $T_2$  relaxation time was significantly lower in seed mucilage than in root mucilage (Figure 3d). Except for flax seed mucilage, the purification significantly reduced the  $T_2$  relaxation time. For chia seed and wheat root mucilage, this effect was significantly stronger with ethanol precipitation than with dialysis.

## 4 | DISCUSSION

### 4.1 | The role of supramolecular interactions for physical properties

In order to understand how the chemical mucilage properties determine the supramolecular polymer interactions which affected the changes in physical mucilage properties upon the purification treatments, a correlation matrix is presented that shows the correlation coefficients  $r$  with  $p$  values below 0.1 (Figure 4). While in the following the interpretation is summarized, these aspects are discussed more detailed in the Supporting information (SI chapter 2).

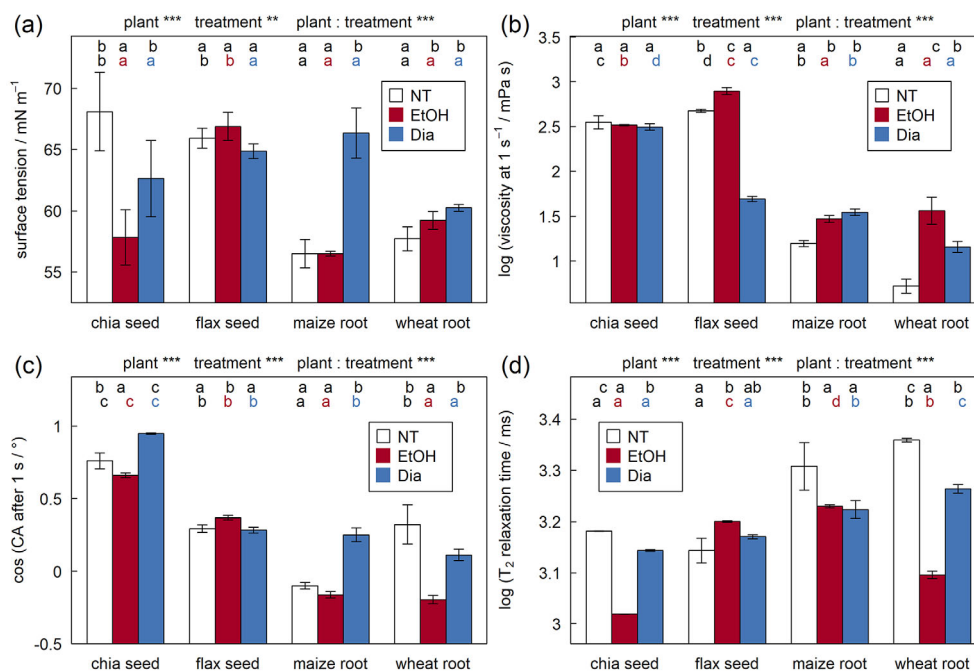


**FIGURE 3** (a) Surface tension, (b) logarithmic apparent viscosity at a shear rate of  $1 \text{ s}^{-1}$ , (c) wettability as cosine of sessile drop contact angle at a drop age of 1 s on dried mucilage, and (d) water mobility expressed as logarithmic transverse  $^1\text{H}$  relaxation time  $T_2$  of non-treated (NT), dialysed (Dia) and ethanol precipitated (EtOH) mucilage in a concentration of 0.3 weight%. Same letters above the bars in the first line indicate no significant differences between treatments of mucilage within one plant, while same letters in the same color in the second line indicate no significant differences between mucilage of different plants within one treatment. Error bars represent standard errors of replicates.

#### 4.1.1 | Cationic interactions enhance viscosity and water retention

The negative correlation of the dialysis yield with pH of NT samples (Figure 4a, Figure S3) indicate that a higher number of acidic groups allows for more cross-links with multivalent cations that cause larger inter- and intra-molecular mucilage assemblies. The positive correlation of viscosity and negative correlation of  $T_2$  relaxation time with Ca and Mg in the strongly bound fraction F3 (Figure 4a, Figure S5a,b) show that viscosity of mucilage depends on the stabilization of the polymer network by multivalent cations and the resulting reduced mesh size of the network may thus restrict water stronger.<sup>[18,32,33]</sup> Viscosity also increased with decreasing K content in F3 (Figure 4a, Figure S5) which indicates that K interacted preferentially with acidic groups that cannot be cross-linked and that are energetically less favorable for multivalent cations because the next acidic group for a cross-link is too far away.<sup>[34]</sup>

#### 4.1.2 | Hydrophobic interactions lower surface tension and wettability

Increasing EtOH yield with decreasing Dia yield (Figure 4d) and thus with increasing amount of low molecular weight (LMW) substances suggests that obviously not the size but the polarity of the polymers determine the EtOH yield.<sup>[16]</sup> Increasing EtOH yield with decreasing original (NT) surface tension and with a trend of decreasing original wettability (Figure 4a, Figure S3c,d) indicate that the lower the polarity of the

polymers the more hydrophobic interactions may be formed which is further supported by the presence of surfactants.<sup>[35]</sup> The overall negative correlation of viscosity with  $T_2$  relaxation time in NT and Dia but not in EtOH samples (Figure 4a-c, Figure S4c) suggest that water retention in the latter was to a higher degree caused by weaker hydrophobic interactions. These interactions dissociate easier under shear force and thus result in a lower viscosity than cationic cross-links.

#### 4.1.3 | Substance exchange is hindered by cationic cross-links

Viscosity correlated positively with surface tension and negatively with EC (Figure 4a, Figure S4d,f) indicating that the better the polymers were cross-linked the more hindered was the migration of mobile charge carriers and the diffusion of surface-active substances to the surface.<sup>[36]</sup> Also, wettability of dried mucilage generally increased with increasing viscosity, with highest significance for Dia samples (Figure 4c, d, Figure S4e) suggesting that the reduced mobility of surface-active substances mitigated a surface hydrophobization during drying.<sup>[37]</sup>

### 4.2 | Differences in seed and root mucilage's physical behavior based on their chemical properties

Seed mucilage exhibits characteristics of acidic polysaccharides connected by multivalent cationic interactions, forming a dense and



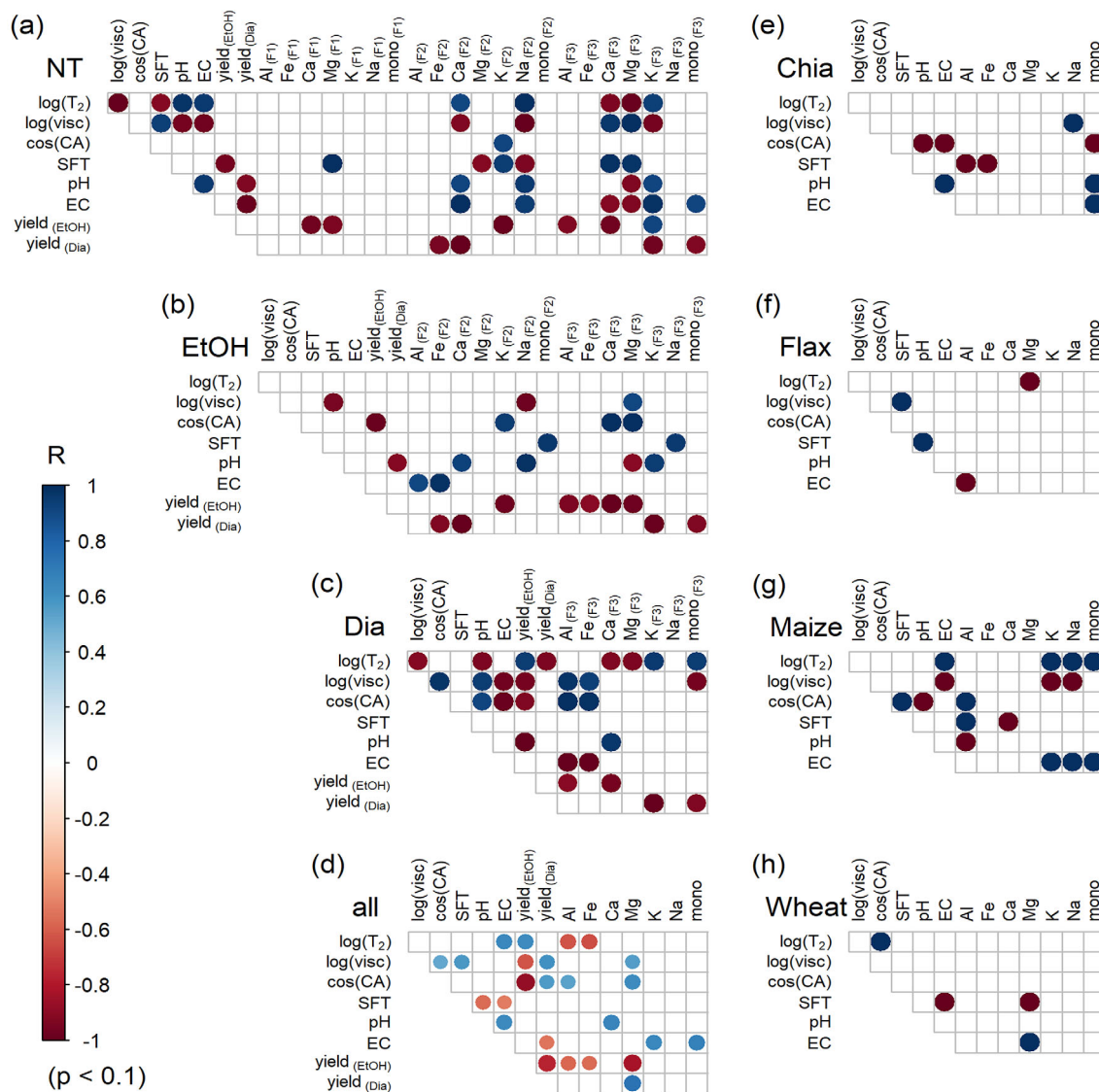


**FIGURE 4** Treatment-wise correlation plots for water mobility expressed as logarithmic transverse  $^1\text{H}$  relaxation time  $T_2$  ( $\log(T_2)$ ), logarithmic apparent viscosity at  $1\text{ s}^{-1}$  shear rate ( $\log(\text{visc})$ ), wettability as cosine of sessile drop contact angle after a drop age of 1 s on dried mucilage ( $\cos(\text{CA})$ ), pH, electrical conductivity (EC), ethanol precipitation yield ( $\text{yield}_{(\text{EtOH})}$ ), dialysis yield ( $\text{yield}_{(\text{Dia})}$ ), content of aluminum (Al), iron (Fe), calcium (Ca), magnesium (Mg), potassium (K), and sodium (Na) content, and the ratio of mono- to bivalent cations (mono) in three different fractions, the ethanol soluble fraction (F1), the ethanol insoluble fraction  $<12\text{--}14\text{ kDa}$  (F2) and the fraction  $>12\text{--}14\text{ kDa}$  for chia and flax seed and maize and wheat root mucilage (a) for the non-treated samples (NT), (b) for the ethanol precipitated samples (EtOH), (c) for the dialyzed samples (Dia), and (d) for all samples together, and plant-wise correlation plots for (e) chia seed, (f) flax seed, (g) maize root, and (h) wheat root mucilage. Color of the dots corresponds to the correlation coefficient  $R$  as shown in the legend. Correlations are considered significant for  $p$  values  $<0.1$ .

stable network. This dense network results in higher viscosity, leading to reduced mobility of surface-active substances and ions, which contributes to higher surface tension and lower EC compared to root mucilage. The higher density of acidic groups in seed mucilage allows for more crosslinks through multivalent cations, restricting cation mobility and lowering EC, despite the higher content of “free cations” in fraction F1 of seed mucilage compared to root mucilage. This is also evident in the lower  $T_2$  relaxation time (Figure 3d), indicating stronger water retention within the polymer network of seed mucilage compared to root mucilage. Consistent with this, the slower solute transport through soil amended with chia seed mucilage, due to the

presence of a higher amount of immobile water, supports the stronger cross-linked polymer network of seed mucilage compared to wheat root mucilage.<sup>[38]</sup> The stronger cross-linking likely renders seed mucilage more resistant to environmental changes but less flexible in responding to these changes with alterations in physical properties. This is reflected in the smaller changes in viscosity and wettability observed upon purification of chia seed mucilage and in the properties of flax seed mucilage, including SFT, wettability, and  $T_2$  relaxation time, compared to root mucilage types (Figure 3a-d).

In contrast, root mucilage is characterized by smaller, less polar, and less acidic polysaccharides, resulting in a looser network. The

higher  $T_2$  relaxation time and lower viscosity of root mucilage indicate lower water retention but easier spreading on surfaces after exudation compared to seed mucilage. This is supported by the positive correlation of viscosity and the negative correlation of the  $T_2$  relaxation time with monovalent cations in maize root mucilage, which are in concurrence to multivalent cross-linkers (Figure 4g, Figure S10c–f). For wheat mucilage, wettability is negatively correlated with viscosity and positively correlated with water mobility, while surface tension negatively correlates with EC and Mg content (Figure 4h, Figure S11a–d). This suggests that the higher flexibility of the wheat root mucilage network enhances wettability through faster rearrangement of hydrophilic polymer components during the re-swelling process, while surface tension increases with the depletion of cations and surfactants. In contrast, for maize mucilage, wettability and surface tension are positively correlated (Figure 4g, Figure S11e). This indicates that the hydrophobic behavior of maize mucilage is mainly caused by amphiphiles in fraction F2 that accumulate at the surface during drying. These amphiphiles likely remained after ethanol precipitation but were removed during dialysis, resulting in improved wettability (Figure 3a,c).

## 5 | CONCLUSIONS: SEED AND ROOT MUCILAGE'S ABILITY TO RESPOND TO CHANGING RHIZOSPHERE CONDITIONS

The discussed differences in chemical and resulting physical properties of seed and root mucilage, as well as their responsiveness to environmental changes, can be attributed to their distinct functions in the rhizosphere. A comprehensive review by Tsai et al.<sup>[39]</sup> describes the functions ascribed to seed mucilage, which can be summarized as seed dispersal, fixation, and protection against abiotic stress. The high viscosity of seed mucilage contributes to its adhesive properties, enabling it to stick to soil particles and safeguard the seed from being washed away by heavy rain or wind.<sup>[40,41]</sup> Seed mucilage also exhibits protective qualities during dispersal, such as resistance against digestion in the digestive tract of animals.<sup>[42,43]</sup> This protective barrier acts against aggressive substances, aligning with our finding that substance mobility is significantly reduced within the seed mucilage network. Moreover, seed mucilage effectively retains water within its structure during soil drying,<sup>[44]</sup> functioning as a water reservoir rather than facilitating water conduction and uptake by the seed.<sup>[45]</sup> Consequently, seed mucilage acts as a physical barrier, impeding the diffusion of water, oxygen, and salt, thereby preventing germination under unfavorable environmental conditions.<sup>[46]</sup> This suggests that seed mucilage plays a crucial role in protecting the seedling during germination, relying on stored substances within the seed rather than external nutrient exchange.

In contrast, root mucilage requires the mobility of water, surfactants, and ions to facilitate their transport through the rhizosphere soil to the root surface. Our findings strongly indicate that the less tightly cross-linked network of root mucilage allows it to be more adaptable to changing environmental conditions. Although

hydrophobic interactions are weaker, they possess self-healing potential: after mechanical stress, such as acting as a lubricant during root penetration into soil pores, hydrophobic interactions reform due to self-organizing processes supported by the presence of surfactants.<sup>[17]</sup> The high flexibility of the network provides root mucilage with several properties that support plant growth. When wet, root mucilage's reduced surface tension allows it to spread on surrounding soil particles and increase the root-soil interface.<sup>[47]</sup> Unlike seed mucilage, the looser network of root mucilage enables the transport of water and solutes from the rhizosphere soil to the root surface, enhancing nutrient availability for plants. As mucilage dries, its viscosity increases, enhancing water retention, and the accumulation of surface-active substances reduces its wettability.<sup>[48]</sup> This increased repellency and viscosity of root mucilage likely contribute to the formation of “liquid bridges”, such as filaments or hollow cylinders, between rhizosphere soil particles.<sup>[49]</sup> This enhances soil structural stability and maintains hydraulic connectivity between the root and soil,<sup>[3]</sup> facilitating nutrient diffusion in a drying rhizosphere.<sup>[50]</sup> The repellent properties of root mucilage after drying also slow down the rewetting of the rhizosphere,<sup>[51]</sup> preventing rapid water entry that could lead to slaking of the rhizosphere structure.<sup>[52]</sup>

To verify the interpretation of the presented results, additional chemical information on the different types of mucilage is required. It is necessary to examine the polysaccharide composition, including the presence of various sugar monomers and their linkages, as well as the contribution of uronic acids and deoxy sugars. Furthermore, analyzing the molecular weight, size distribution of the mucilage polymers, and understanding the relationship between the chemical composition, molecular interactions, and physical properties of mucilage will aid in validating the findings. Additionally, studying the reversibility of the observed changes under more realistic conditions is essential to comprehend how alterations in the rhizosphere's environmental conditions may affect these physical properties and enable their specific ecological functions.

## ACKNOWLEDGMENTS

This study was carried out in the framework of the priority program 2089 Rhizosphere-spatiotemporal organization—a key to rhizosphere functions and funded by the German Research Foundation DFG under the project number 403668613. We further want to thank Jana auf der Landwehr and Anna Baskal who contributed to the laboratory analyses. Open Access funding enabled and organized by Projekt DEAL.

## CONFLICT OF INTEREST STATEMENT

The authors declare that they have no known competing financial interests or personal relationships that could have appeared to influence the work reported in this paper.

## DATA AVAILABILITY STATEMENT

The data supporting the results of this study are available in the repository “figshare” under <https://doi.org/10.6084/m9.figshare.23101415>.

## ORCID

Doerte Diehl  <https://orcid.org/0000-0001-6868-3627>Gabriele E. Schaumann  <https://orcid.org/0000-0003-1788-2751>

## REFERENCES

- [1] J. W. Crawford, L. Deacon, D. Grinev, J. A. Harris, K. Ritz, B. K. Singh, I. Young, *J. R. Soc. Interface* **2012**, *9*, 1302.
- [2] A. Carminati, A. B. Moradi, D. Vetterlein, P. Vontobel, E. Lehmann, U. Weller, H.-J. Vogel, S. E. Oswald, *Plant Soil* **2010**, *332*, 163.
- [3] A. Carminati, *Vadose Zone J.* **2012**, *11*, vj2011.0106.
- [4] E. Kroener, M. Zarebanadkouki, A. Kaestner, A. Carminati, *Water Resources Res.* **2014**, *50*, 6479.
- [5] P. D. Hallett, *Soil Water Res* **2008**, *3*, 21.
- [6] A. B. Moradi, A. Carminati, A. Lamparter, S. K. Woche, J. Bachmann, D. Vetterlein, H.-J. Vogel, S. E. Oswald, *Vadose Zone J.* **2012**, *11*, e0120.
- [7] D. B. Read, A. G. Bengough, P. J. Gregory, J. W. Crawford, D. Robinson, C. M. Scrimgeour, I. M. Young, K. Zhang, X. Zhang, *New Phytol.* **2003**, *157*, 315.
- [8] I. Gholamali, *Regen. Eng. Transl. Med.* **2021**, *7*, 91.
- [9] M. S. Erich, B. R. Hoskins, *Commun. Soil Sci. Plant Anal.* **2011**, *42*, 1167.
- [10] M. Kim, D. Or, *Nat. Commun.* **2019**, *10*, 3944.
- [11] M. Diener, J. Adamcik, A. Sánchez-Ferrer, F. Jaedig, L. Schefer, R. Mezzenga, *Biomacromolecules* **2019**, *20*, 1731.
- [12] Y. Huang, Y. Wang, L. Sun, R. Agrawal, M. Zhang, *J. R. Soc. Interface* **2015**, *12*, 20150226.
- [13] M. Brax, G. E. Schaumann, D. Diehl, *J. Plant Nutr. Soil Sci.* **2019**, *182*, 92.
- [14] M. Tako, *Adv. Biosci. Biotechnol.* **2015**, *6*, 15.
- [15] M. F. Akhtar, M. Hanif, N. M. Ranjha, *Saudi Pharm. J.* **2016**, *24*, 554.
- [16] M. Q. Guo, X. Hu, C. Wang, L. Ai, in *Solubility of Polysaccharides* (Ed: Z. Xu), InTech, Vienna, Austria **2017**. <https://doi.org/10.5772/intechopen.71570>
- [17] D. C. Tuncaboylu, M. Sahin, A. Argun, W. Oppermann, O. Okay, *Macromolecules* **2012**, *45*, 1991.
- [18] G. Stojkov, Z. Niyazov, F. Picchioni, R. K. Bose, *Gels* **2021**, *7*, 255.
- [19] T. Kopač, M. Abrami, M. Grassi, A. Ručigaj, M. Krajnc, *Carbohydr. Polym.* **2022**, *277*, 118895.
- [20] G. E. Schaumann, D. Gildemeister, Y. Kunhi Mouvenchery, S. Spielvogel, D. Diehl, *J. Soils Sediments* **2013**, *13*, 1579.
- [21] M. Brax, C. Buchmann, K. Kenngott, G. E. Schaumann, D. Diehl, *Bio-geochemistry* **2020**, *147*, 35.
- [22] S. Meiboom, D. Gill, *Rev. Sci. Instrum.* **1958**, *29*, 688.
- [23] R Core Team. R: A Language and Environment for Statistical Computing. **2020**. <https://www.R-project.org/>
- [24] A. Daerr, A. Mogne, *J. Open Res. Softw.* **2016**, *4*, e3.
- [25] C. A. Schneider, W. S. Rasband, K. W. Eliceiri, *Nat. Methods* **2012**, *9*, 671.
- [26] R. Kaltenbach, D. Diehl, G. E. Schaumann, *J. Colloid Interface Sci.* **2018**, *516*, 446.
- [27] D. Bates, M. Mächler, B. Bolker, S. Walker, *J. Stat. Softw.* **2015**, *67*, 48.
- [28] A. Kuznetsova, P. B. Brockhoff, R. H. B. Christensen. lmerTest: Tests in Linear Mixed Effects Models. **2016**. <https://CRAN.R-project.org/package=lmerTest>
- [29] T. Hothorn, F. Bretz, P. Westfall, *Biom. J.* **2008**, *50*, 346.
- [30] J. Fox, S. Weisberg, *An R Companion to Applied Regression*, 2nd ed., SAGE Publications, Thousand Oaks **2011**.
- [31] X. Yan, *J. AOAC Int.* **2017**, *100*, 1134.
- [32] M. Brax, C. Buchmann, G. E. Schaumann, *J. Plant Nutr. Soil Sci.* **2017**, *180*, 121.
- [33] A. H. Karoyo, L. D. Wilson, *Materials* **2021**, *14*, 1095.
- [34] G. E. Schaumann, Y. Kunhi Mouvenchery, *J. Plant Nutr. Soil Sci.* **2018**, *181*, 441.
- [35] H. Bao, L. Li, L. H. Gan, H. Zhang, *Macromolecules* **2008**, *41*, 9406.
- [36] E. Axpe, D. Chan, G. S. Offeddu, Y. Chang, D. Merida, H. L. Hernandez, E. A. Appel, *Macromolecules* **2019**, *52*, 6889.
- [37] M. Knott, M. Ani, E. Kroener, D. Diehl, *Plant Soil* **2022**, *478*, 85.
- [38] A. Paporisch, H. Bavli, R. J. Strickman, R. B. Neumann, N. Schwartz, *Water Resour. Res.* **2021**, *57*, e2021WR029976.
- [39] A. Y.-L. Tsai, R. McGee, G. H. Dean, G. W. Haughn, S. Sawa, *Plant Cell Physiol.* **2021**, *62*, 1847.
- [40] J. Akhtar, A. F. Galloway, G. Nikolopoulos, K. J. Field, P. Knox, *Plant Soil* **2018**, *428*, 57.
- [41] M. Engelbrecht, E. Bochet, P. Garcia-Fayos, *Biol. J. Linn. Soc.* **2014**, *111*, 241.
- [42] X. Yang, J. M. Baskin, C. C. Baskin, Z. Huang, *Perspect. Plant Ecol. Evol. Syst.* **2012**, *14*, 434.
- [43] A. F. Galloway, P. Knox, K. Krause, *New Phytol.* **2020**, *225*, 1461.
- [44] M. Naveed, M. A. Ahmed, P. Benard, L. K. Brown, T. S. George, A. G. Bengough, T. Roose, N. Koebernick, P. D. Hallett, *Plant Soil* **2019**, *437*, 65.
- [45] S. Saez-Aguayo, C. Rondeau-Mouro, A. Macquet, I. Kronholm, M.-C. Ralet, A. Berger, C. Sallé, D. Poulain, F. Granier, L. Botran, O. Loudet, J. d. Meaux, A. Marion-Poll, H. M. North, *PLoS Genet.* **2014**, *10*, e1004221.
- [46] M. Gorai, W. El Aloui, X. J. Yang, M. Neffati, *Plant Soil* **2014**, *374*, 727.
- [47] D. B. Read, P. J. Gregory, *New Phytol.* **1997**, *137*, 623.
- [48] M. A. Ahmed, E. Kroener, P. Benard, M. Zarebanadkouki, A. Kaestner, A. Carminati, *Plant Soil* **2016**, *407*, 161.
- [49] P. Benard, M. Zarebanadkouki, C. Hedwig, M. Holz, M. A. Ahmed, A. Carminati, *Vadose Zone J.* **2018**, *17*, 1.
- [50] M. Zarebanadkouki, T. Fink, P. Benard, C. C. Banfield, *Vadose Zone J.* **2019**, *18*, 190021.
- [51] P. Benard, E. Kroener, P. Vontobel, A. Kaestner, A. Carminati, *Adv. Water Resour.* **2016**, *95*, 190.
- [52] C. Buchmann, J. Bentz, G. E. Schaumann, *Soil Tillage Res.* **2015**, *154*, 22.

## SUPPORTING INFORMATION

Additional supporting information can be found online in the Supporting Information section at the end of this article.

**How to cite this article:** Diehl, M. Knott, G. E. Schaumann, *Biopolymers* **2023**, *114*(8), e23561. <https://doi.org/10.1002/bip.23561>